

Synthesis of the Reagent $[\text{Na}][\text{Pt}(\text{PEt}_3)_2(\eta^5\text{-7-CB}_{10}\text{H}_{11})]$ and Preparation of the Platinacarborane Complexes $[\text{PtX}(\text{PEt}_3)_2(\eta^5\text{-7-CB}_{10}\text{H}_{11})]$ (X = H, Au(PPh₃), Cu(PPh₃), HgPh)[†]

Stewart A. Batten,[‡] John C. Jeffery,[‡] Peter L. Jones,[‡] Donald F. Mullica,[§] Martin D. Rudd,[§] Eric L. Sappenfield,[§] F. Gordon A. Stone,^{*,§} and Andreas Wolf[§]

Department of Chemistry, Baylor University, Waco, Texas 76798-7348, and School of Chemistry, The University, Bristol BS8 1TS, U.K.

Received January 15, 1997[⊗]

The salt $[\text{Na}][\text{Pt}(\text{PEt}_3)_2(\eta^5\text{-7-CB}_{10}\text{H}_{11})]$ (**1a**) has been prepared. Protonation affords the hydrido complex $[\text{PtH}(\text{PEt}_3)_2(\eta^5\text{-7-CB}_{10}\text{H}_{11})]$ (**2**) while reactions with $[\text{AuCl}(\text{PPh}_3)]$, $[\text{CuCl}(\text{PPh}_3)]_4$, and $[\text{HgClPh}]$ yield the dimetal compounds $[\text{PtM}(\text{PEt}_3)_2(\text{PPh}_3)(\eta^5\text{-7-CB}_{10}\text{H}_{11})]$ (**3a**, M = Au; **3b**, M = Cu) and $[\text{PtHgPh}(\text{PEt}_3)_2(\eta^5\text{-7-CB}_{10}\text{H}_{11})]$ (**3c**), respectively. The salt $[\text{N}(\text{PPh}_3)_2][\text{Pt}(\text{CO})(\text{PPh}_3)(\eta^5\text{-7-CB}_{10}\text{H}_{11})]$ (**4**) has also been obtained. Single-crystal X-ray diffraction studies have been made on **2** and **3a–c**. Complexes **2**, **3a**, and **3c** have similar molecular structures with H, Au(PPh₃), and HgPh groups, respectively, σ -bonded to the Pt of the $\text{Pt}(\text{PEt}_3)_2(\eta^5\text{-7-CB}_{10}\text{H}_{11})$ group. In **3b**, however, the copper atom of the Cu(PPh₃) moiety is attached to the $\text{Pt}(\text{PEt}_3)_2(\eta^5\text{-7-CB}_{10}\text{H}_{11})$ fragment both by a Pt–Cu σ -bond and by two exopolyhedral B–H→Cu donor bonds from BH groups in the open face of the *nido*-7-CB₁₀H₁₁ cage ligating the platinum. The structure of the salt **4** has also been determined by X-ray diffraction.

Introduction

Relatively few monocarbon metallacarboranes are known whereas substantial numbers of dicarbon metallacarboranes have been prepared.¹ Thus, whereas several platinacarborane complexes with *closo*-PtC₂B₉ cage frameworks have been well characterized,^{2–6} as far as we are aware there are only two known monocarbon carborane–platinum compounds with *closo*-icosahedral structures: $[\text{NMe}_4][\text{Pt}(\text{PEt}_3)_2(\eta^5\text{-7-CB}_{10}\text{H}_{11})]$ and $[\text{Pt}(\text{PEt}_3)_2(\eta^5\text{-7-NMe}_3\text{-7-CB}_{10}\text{H}_{10})]$. Both complexes were synthesized by polyhedral expansion reactions⁷ involving treatment of $[\text{NMe}_4][\text{closo-CB}_{10}\text{H}_{11}]$ and *closo*-7-NMe₃-CB₁₀H₁₀, respectively, with $[\text{Pt}(\text{PEt}_3)_2(\text{trans-PhC}(\text{H})=\text{C}(\text{H})\text{Ph})]$.⁸ Further studies on species containing a *closo*-2,1-PtCB₁₀H₁₁ framework are

warranted since the CB₁₀H₁₁ group present in the anion $[\text{Pt}(\text{PEt}_3)_2(\eta^5\text{-7-CB}_{10}\text{H}_{11})]^-$ formally donates three electrons to the platinum atom whereas in the isolobal neutral complex $[\text{Pt}(\text{PEt}_3)_2(\eta^5\text{-7,8-C}_2\text{B}_9\text{H}_{11})]$ ^{2a} the carborane ligand contributes four electrons. Different reactivity patterns are likely to result. Thus, whereas $[\text{Pt}(\text{PEt}_3)_2(\eta^5\text{-7,8-C}_2\text{B}_9\text{H}_{11})]$ is unreactive at the platinum center the anionic complex $[\text{Pt}(\text{PEt}_3)_2(\eta^5\text{-7-CB}_{10}\text{H}_{11})]^-$ should be sufficiently nucleophilic to protonate to afford a hydride or react with certain metal halides to generate species with bonds between platinum and other metals. For this reason we have prepared the salt $[\text{Na}][\text{Pt}(\text{PEt}_3)_2(\eta^5\text{-7-CB}_{10}\text{H}_{11})]$ (**1a**) and have studied some reactions of this compound.

Results and Discussion

A thf (tetrahydrofuran) suspension of $[\text{Na}]_3[\text{nido-CB}_{10}\text{H}_{11}]$, obtained from *nido*-7-Me₃N-7-CB₁₀H₁₂,⁹ was treated with $[\text{PtCl}_2(\text{PEt}_3)_2]$ to give an orange-brown solution of $[\text{Na}][\text{Pt}(\text{PEt}_3)_2(\eta^5\text{-7-CB}_{10}\text{H}_{11})]$ (**1a**) (Chart 1). The salt contains small amounts of $[\text{Na}][\text{nido-CB}_{10}\text{H}_{13}]$ as an impurity and is readily protonated (see below). It was therefore generally freshly prepared and used *in situ*. Solutions of the potassium salt **1b** in thf were obtained in a similar manner.

Addition of HBF₄·Et₂O to a thf solution of **1a** gave colorless crystals of $[\text{PtH}(\text{PEt}_3)_2(\eta^5\text{-7-CB}_{10}\text{H}_{11})]$ (**2**) characterized by the data given in Tables 1 and 2. The ¹H NMR spectrum shows a diagnostic signal for the hydrido ligand at δ –8.78, appearing as a triplet with ¹⁹⁵Pt satellite peaks [$J(\text{PH}) = 27$, $J(\text{PtH}) = 1030$ Hz]. There was also a resonance at δ 2.79 for the cage CH group. A signal characteristic for the latter appears in the ¹³C{¹H} NMR spectrum at δ 50.9. The ³¹P{¹H} NMR spectrum displays a singlet at δ 8.7 ($J(\text{PtP}) = 1817$ Hz). Complex **2** readily forms from **1a** if solutions of the latter are chromatographed on silica gel. Deprotonation of **2** with $[\text{K}(\text{BH}(\text{CHMeEt})_3)]$ afforded **1b** free of any $[\text{K}(\text{CB}_{10}\text{H}_{13})]$ impurity, thus allowing the ¹H and ¹¹B{¹H} NMR data for **1b** to be obtained (Table 2) in the absence of signals due to the anion $[\text{CB}_{10}\text{H}_{13}]^-$.

[†] The complexes described in this paper have a platinum atom incorporated into a *closo*-1-carba-2-platnadodecaborane structure. However, to avoid a complicated nomenclature for the compounds reported, and to relate them to species with η^5 -coordinated cyclopentadienyl ligands, following precedent (Jeffery, J. C.; Sappenfield, E. L.; Lebedev, V. N.; Stone, F. G. A. *Inorg. Chem.* **1996**, *35*, 2967), we treat the cages as *nido*-11-vertex ligands with numbering as for an icosahedron from which the twelfth vertex has been removed.

[‡] University of Bristol.

[§] Baylor University.

[⊗] Abstract published in *Advance ACS Abstracts*, May 1, 1997.

- (1) Grimes, R. N. In *Comprehensive Organometallic Chemistry II*; Abel, E. W., Stone, F. G. A., Wilkinson, G., Eds.; Pergamon Press: Oxford, U.K., 1995; Vol. 1 (Housecroft, C. E., Ed), Chapter 9.
- (2) Warren, L. F.; Hawthorne, M. F. *J. Am. Chem. Soc.* **1970**, *92*, 1157.
- (3) (a) Green, M.; Spencer, J. L.; Stone, F. G. A.; Welch, A. J. *J. Chem. Soc., Dalton Trans.* **1975**, 179. (b) Carr, N.; Mullica, D. F.; Sappenfield, E. L.; Stone, F. G. A. *Inorg. Chem.* **1994**, *33*, 1666.
- (4) Graham, W. A. G.; Krentz, R. Unpublished results. See: Krentz, R. Ph.D. Thesis, University of Alberta, 1989.
- (5) (a) Mingos, D. M. P.; Forsyth, M. I.; Welch, A. J. *J. Chem. Soc., Dalton Trans.* **1978**, 1363. (b) Baghurst, D. R.; Copley, R. C. B.; Fleischer, H.; Mingos, D. M. P.; Kyd, G. O.; Yellowlees, L. J.; Welch, A. J.; Spalding, T. R.; O'Connell, D. *J. Organomet. Chem.* **1993**, *447*, C14.
- (6) Colquhoun, H. M.; Greenhough, Wallbridge, M. G. H. *J. Chem. Soc., Dalton Trans.* **1985**, 761. Alcock, N. W.; Taylor, J. G.; Wallbridge, M. G. H. *J. Chem. Soc., Dalton Trans.* **1987**, 1805.
- (7) Stone, F. G. A. *J. Organomet. Chem.* **1975**, *100*, 257.
- (8) Carroll, W. E.; Green, M.; Stone, F. G. A.; Welch, A. J. *J. Chem. Soc., Dalton Trans.* **1975**, 2263.

(9) Knoth, W. H.; Little, J. L.; Lawrence, J. R.; Scholer, F. R.; Todd, L. *J. Inorg. Synth.* **1968**, *11*, 33.

Table 1. Analytical and Physical Data

compd ^b	color	yield/%	anal./% ^a	
			C	H
[PtH(PEt ₃) ₂ (η ⁵ -7-CB ₁₀ H ₁₁)] (2)	off-white	65	28.4 (27.7)	7.9 (7.5)
[PtAu(PEt ₃) ₂ (PPh ₃)(η ⁵ -7-CB ₁₀ H ₁₁)] (3a)	pale tan	51	36.2 (36.4)	5.5 (5.5)
[PtCu(PEt ₃) ₂ (PPh ₃)(η ⁵ -7-CB ₁₀ H ₁₁)] (3b)	pale yellow	47	42.1 (41.9)	6.3 (6.3)
[PtHg(Ph)(PEt ₃) ₂ (η ⁵ -7-CB ₁₀ H ₁₁)] (3c)	yellow	56	27.0 (27.2)	5.2 (5.5)
[N(PPh ₃) ₂][Pt(CO)(PPh ₃)(η ⁵ -7-CB ₁₀ H ₁₁)] (4)	orange	5	54.9 (55.2) ^c	4.9 (4.7)

^a Calculated values are given in parentheses. ^b All compounds show very broad medium intensity bands in their infrared spectra, measured in CH₂Cl₂, at ca. 2550 cm⁻¹ due to B–H absorptions. There is also a strong band at 2019 cm⁻¹ for the CO group of **4**. ^c Crystallizes with 1 molecule of CH₂Cl₂.

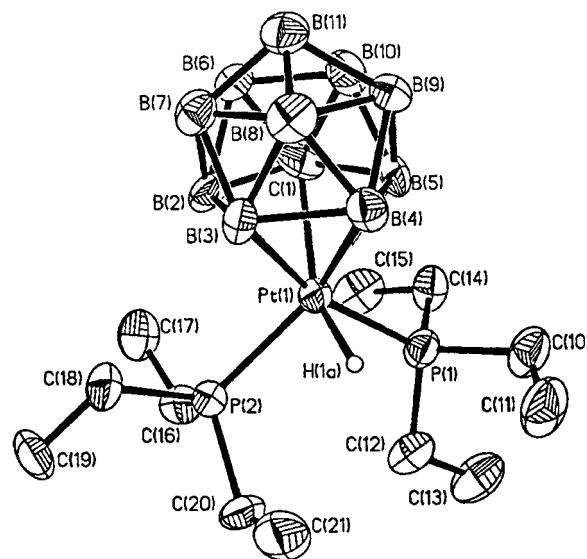
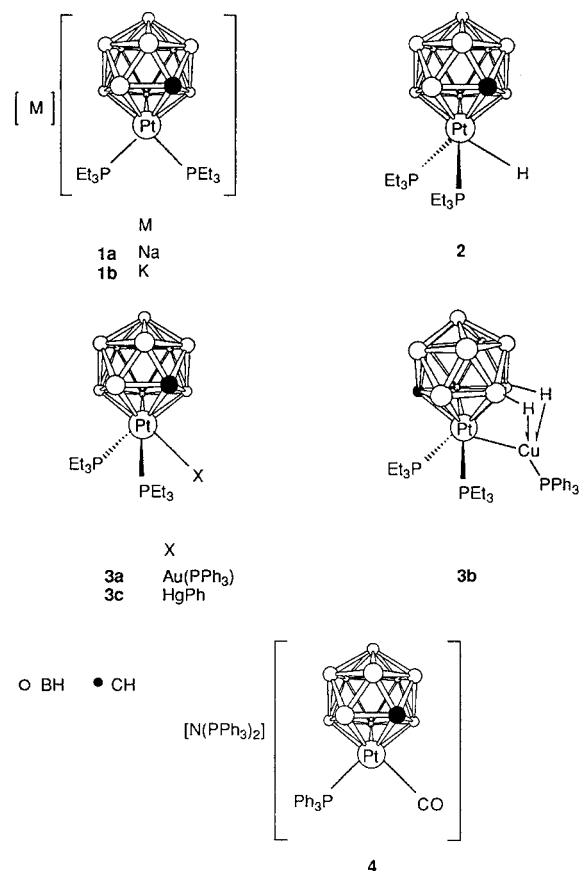
Chart 1

Figure 1. Molecular structure of [PtH(PEt₃)₂(η⁵-7-CB₁₀H₁₁)] (**2**), showing the crystallographic labeling scheme. Thermal ellipsoids are at the 40% probability level, and except for H(1A) hydrogen atoms are omitted for clarity.

Selected bond distances and angles from an X-ray diffraction study on **2** are listed in Table 3, and the molecule is shown in Figure 1. The hydrido ligand H(1A) was not located in an electron-density difference map, but its position was found by employing the steric potential energy minimization technique.¹⁰ The Pt(1)–H(1A) separation (1.596 Å) derived by this method is very close to that (1.610(2) Å) for the terminal hydrido ligand in [Pt₂H(*μ*-H)₂(Ph₂PCH₂CH₂PPh₂)₂][BPh₄] determined by neutron diffraction¹¹ but somewhat shorter than that (1.66 Å) reported for [PtH(PEt₃)₂(*nido*-η⁴-7-SB₉H₁₀)].¹² The open face of the *nido*-CB₁₀H₁₁ cage in **2** is pentahapto coordinated to the platinum (Pt(1)–C(1) = 2.305(10), Pt(1)–B(2) = 2.279(13), Pt(1)–B(3) = 2.258(14), Pt(1)–B(4) = 2.244(12), Pt(1)–B(5) = 2.217(9) Å). One other molecule in which a Pt atom is η⁵-coordinated to a CBBBB ring with the carbon vertex bonded to a hydrogen atom has been studied crystallographically: [Pt-(PMe₂Ph)₂(η⁵-8-Ph-2,8-C₂B₉H₁₀)].^{5b} In the latter species the

Pt–C distance (2.581(4) Å) is somewhat longer, but the Pt–B connectivities are in a range similar (2.21–2.28 Å) to those in **2**. The X-ray diffraction study of the zwitterionic palladium complex [Pd(CNBU₃)₂(η⁵-7-Me₃N-7-CB₁₀H₁₀)]⁸ revealed a Pd–C distance of 2.600(6) Å, appreciably longer than the Pt–C distance in **2** although the covalent radii of Pd and Pt are the same. However, the Pd–B connectivities are comparable, so the longer metal to cage-carbon distance in the palladium species is probably due to a steric effect resulting from the presence of the NMe₃ substituent on the carbon.^{5b} The two Pt–P bond lengths in **2** are essentially the same (average 2.362 Å) and correspond closely with the average (2.385 Å) found in six-coordinate platinum complexes having Pt(PEt₃)₂ groups.¹³

Addition of thf solutions of [AuCl(PPh₃)] and [CuCl(PPh₃)]₄, respectively, to solutions of **1a** in the same solvent cooled to low temperatures afforded the crystalline complexes [PtM-(PEt₃)₂(PPh₃)(η⁵-7-CB₁₀H₁₁)] (**3a**, M = Au; **3b**, M = Cu). Data characterizing these compounds are listed in Tables 1 and 2, but discussion of their NMR spectra is deferred until after the results of the X-ray diffraction studies are described. Although the two molecules have similar compositions, apart from replacement of Au in **3a** by Cu in **3b**, their molecular structures are significantly different.

The structure of **3a** is shown in Figure 2, and selected bond distances and angles are given in Table 4. The platinum atom is ligated on one side by the open pentagonal face of the η⁵-CB₁₀H₁₁ ligand and on the other by two PEt₃ groups and the

(10) Orpen, A. G. *J. Chem. Soc., Dalton Trans.* **1980**, 2509.

(11) Chiang, M. Y.; Bau, R.; Minghetti, G.; Bandini, A. L.; Banditelli, G.; Koetzle, T. F. *Inorg. Chem.* **1984**, *23*, 122.

(12) Kane, A. R.; Guggenberger, L. J.; Muetterties, E. L. *J. Am. Chem. Soc.* **1970**, *92*, 2571.

(13) Orpen, A. G.; Brammer, L.; Allen, F. H.; Kennard, O.; Watson, D. G.; Taylor, R. *J. Chem. Soc., Dalton Trans.* **1989**, S1.

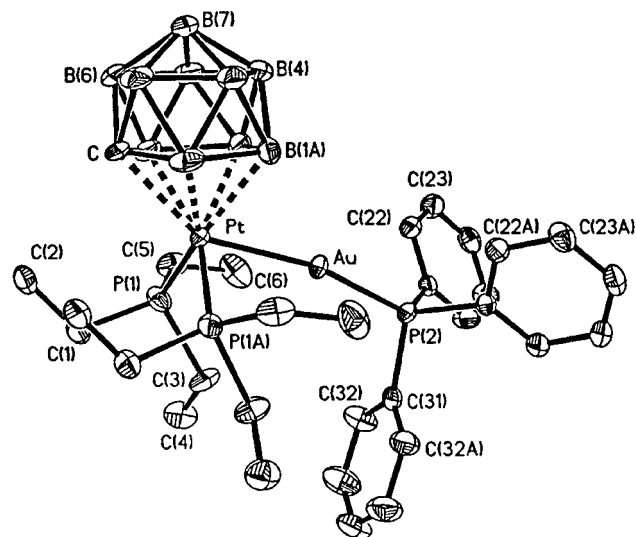
Table 2. Hydrogen-1, Carbon-13, Boron-11, and Phosphorus-31 NMR Data^a

compd	$\delta(^1\text{H})$	$\delta(^{13}\text{C})^b$	$\delta(^{11}\text{B})^c$	$\delta(^{31}\text{P})^d$
1b	1.13 [d of t, 18 H, Me, $J(\text{HH}) = 7$, $J(\text{PH}) = 15$], 1.82 [d of q, 12 H, CH ₂ , $J(\text{HH}) = 8$, $J(\text{PH}) = 15$], 2.41 (s, 1 H cage CH)		-9.4 (3 B), -19.4 (2 B), -21.1 (2 B), -24.5 (3 B)	5.50 [s, $J(\text{PtP}) = 3360$]
2	-8.78 [t, 1 H, PtH, $J(\text{PH}) = 1030$], 1.12 [d of t, 18 H, Me, $J(\text{PH}) = 16$, $J(\text{HH}) = 8$], 2.11 [d of q, 12 H, CH ₂ , $J(\text{HH}) = 7.5$, $J(\text{PH}) = 15$], 2.79 [s, 1 H cage CH]	50.9 (cage CH), 18.8 (m, CH ₂), 8.6 (Me)	11.3 (1 B), -3.8 (4 B, br), -6.4 (1 B), -13.4 (2 B), -17.0 (2 B, br)	8.7 [s, $J(\text{PtP}) = 1817$]
3a	1.05 [d of t, 18 H, Me, $J(\text{HH}) = 8$, $J(\text{PH}) = 16$], 2.06 [d of q, 12 H, CH ₂ , $J(\text{HH}) = 8$, $J(\text{PH}) = 16$], 2.77 (br s, 1 H, cage CH), 7.47-7.58 (m, 15 H, Ph)	134.2-129.3 (m, Ph), 48.2 (s br, cage CH), 22.2 (m, PCH ₂), 14.1 (s, PCH ₂ Me)	4.4 (1 B), -8.1 (4 B, br), -10.0 (1 B), -16.1 (2 B), -18.5 (2 B, br)	38.7 [s, 1 P, PPh ₃ , $J(\text{PtP}) = 498$], 0.6 [s, 2 P, PEt ₃ , $J(\text{PtP}) = 2535$]
3b	0.93 [d of t, 18 H, Me, $J(\text{HH}) = 8$, $J(\text{PH}) = 16$], 1.87 [d of q, 12 H, CH ₂ , $J(\text{HH}) = 8$, $J(\text{PH}) = 16$], 2.93 (br s, 1 H, cage CH), 7.43-7.57 (m, 15 H, Ph)	129.2-134.0 (m, Ph), 52.8 (s br, cage CH), 19.9 (m, PCH ₂), 9.0 (s, PCH ₂ Me)	-1.2 (1 B), -8.5 (1 B), -14.6 (2 B), -17.9 (4 B), -19.2 (2 B)	1.35 [s, 2 P, PEt ₃ , $J(\text{PtP}) = 3147$], 3.32 (br s, 1 P, PPh ₃)
3c	1.23 [d of t, 18 H, Me, $J(\text{HH}) = 7$, $J(\text{PH}) = 16$], 2.21 [d of q, 12 H, CH ₂ , $J(\text{HH}) = 8$, $J(\text{PH}) = 16$], 2.80 (br s, 1 H, cage CH), 7.27-7.41 (m, 5 H, Ph)	128.8-136.1 (m, Ph), 59.3 (br s, cage CH), 21.3 (m, PCH ₂), 9.5 (PCH ₂ Me)	9.2 (1 B), -7.1 (5 B), -14.5 (2 B), -17.1 (2 B)	0.77 [s, $J(\text{PtP}) = 2259$, $^2J(\text{HgP}) = 188$]
4	2.64 (br s, 1 H, cage CH), 7.21-7.67 (m, 45 H, Ph)			13.8 [s, $J(\text{PtP}) = 2288$]

^a Chemical shifts (δ) in ppm, coupling constants (J) in Hz, measurements in CD₂Cl₂ at room temperature. ^b Hydrogen-1 decoupled, chemical shifts are positive to high frequency of SiMe₄. ^c Hydrogen-1 decoupled, chemical shifts are positive to high frequency of BF₃·Et₂O (external). Resonances ascribed to more than one nucleus may result from overlapping signals and do not necessarily indicate symmetry equivalence. ^d Hydrogen-1 decoupled, chemical shifts are positive to high frequency of 85% H₃PO₄ (external).

Table 3. Selected Internuclear Distances (Å) and Angles (deg) for [PtH(PEt₃)₂(η^5 -7-CB₁₀H₁₁)] (**2**), with Estimated Standard Deviations in Parentheses

Pt(1)-H(1A)	1.596	Pt(1)-B(2)	2.279(13)	Pt(1)-B(4)	2.244(12)	Pt(1)-P(1)	2.364(3)
C(1)-B(5)	1.736(13)	C(1)-B(10)	1.654(14)	B(2)-B(3)	1.873(16)	B(2)-B(7)	1.769(20)
B(3)-B(4)	1.837(14)	B(3)-B(8)	1.754(16)	B(4)-B(5)	1.844(18)	B(4)-B(9)	1.782(15)
B(5)-B(9)	1.744(19)	B(6)-B(10)	1.744(16)	B(7)-B(11)	1.764(14)	B(8)-B(9)	1.779(18)
B(9)-B(11)	1.785(18)	B(10)-B(11)	1.725(22)	P(1)-C(10)	1.833(9)	P(1)-C(14)	1.804(11)
P(2)-C(18)	1.846(12)	Pt(1)-C(1)	2.305(10)	Pt(1)-B(3)	2.258(14)	Pt(1)-B(5)	2.217(9)
Pt(1)-P(2)	2.360(2)	C(1)-B(2)	1.725(16)	C(1)-B(6)	1.670(19)	B(2)-B(6)	1.787(16)
B(3)-B(7)	1.755(17)	B(4)-B(8)	1.766(21)	B(5)-B(10)	1.770(18)	B(6)-B(7)	1.777(19)
B(6)-B(11)	1.756(16)	B(7)-B(8)	1.746(14)	B(8)-B(11)	1.782(17)	B(9)-B(10)	1.756(16)
P(1)-C(12)	1.850(12)	P(2)-C(16)	1.815(11)	P(2)-C(20)	1.844(10)		
H(1A)-Pt(1)-P(1)	85.1(1)	H(1A)-Pt(1)-P(2)	86.7(1)	P(1)-Pt(1)-P(2)	98.6(1)	Pt(1)-P(1)-C(10)	112.3(5)
Pt(1)-P(1)-C(12)	118.5(4)	C(10)-P(1)-C(12)	102.2(5)	Pt(1)-P(1)-C(14)	112.6(4)	C(10)-P(1)-C(14)	105.8(4)
C(12)-P(1)-C(14)	104.1(5)	Pt(1)-P(2)-C(16)	118.2(3)	Pt(1)-P(2)-C(18)	112.8(4)	C(16)-P(2)-C(18)	105.9(5)
Pt(1)-P(2)-C(20)	113.1(3)	C(16)-P(2)-C(20)	103.0(5)	C(18)-P(2)-C(20)	102.1(5)		

**Figure 2.** Molecular structure of [PtAu(PEt₃)₂(PPh₃)(η^5 -7-CB₁₀H₁₁)] (**3a**), showing the crystallographic labeling scheme. Thermal ellipsoids are at the 40% probability level, and hydrogen atoms are omitted for clarity.

Au(PPh₃) fragment. The molecule has imposed mirror symmetry with the Pt, Au, C, and P(2) atoms lying on the mirror plane. The Pt-Au distance of 2.6112(7) Å is at the lower end

of the range (2.6-2.9 Å) found for such separations¹⁴ and is considerably shorter than that in [10-*exo*-{Pt(H)(PEt₃)₂}-10-(μ -H)-10-*endo*-{Au(PPh₃)}-7,8-Me₂-*nido*-C₂B₉H₈] (3.000(1) Å) where the gold is directly bonded to the carbaborane fragment and the platinum is exopolyhedrally attached to the cage system via the gold atom and a B-H-Pt three-center two-electron bond.¹⁵ The platinum-to-cage connectivities in **3a** are very similar to those in **2**.

The structure of **3b** is shown in Figure 3, and selected bond distances and angles are given in Table 5. The platinum atom, as expected, is again ligated on one side by the open pentagonal face of the η^5 -CB₁₀H₁₁ ligand and on the other by two PEt₃ groups. However, the Cu(PPh₃) unit is attached to the Pt(PEt₃)₂(η^5 -CB₁₀H₁₁) system not only by a direct Pt-Cu bond (2.6058(5) Å) but by two B-H-Cu bonds involving B(3) and B(4). The Pt-Cu distance is within the range of such distances

- (14) (a) Payne, N. C.; Ramachandran, R.; Schoettel, G.; Vittal, J. J.; Puddephatt, R. J. *Inorg. Chem.* **1991**, *30*, 4048. (b) Ito, L. N.; Felicissimo, A. M. P.; Pignolet, L. H. *Inorg. Chem.* **1991**, *30*, 387. (c) Braunstein, P.; Knorr, M.; Stahrfeldt, T.; Decian, A.; Fischer, J. *J. Organomet. Chem.* **1993**, *459*, C1. (d) Byers, P. K.; Carr, N.; Stone, F. G. A. *J. Chem. Soc., Dalton Trans.* **1990**, 3701. (e) Toronto, D. V.; Balch, A. L. *Inorg. Chem.* **1994**, *33*, 6132. (f) Mingos, D. M. P.; Oster, P.; Sherman, D. J. *J. Organomet. Chem.* **1987**, *320*, 257. (g) Hill, C. M.; Mingos, D. M. P.; Powell, H.; Watson, M. J. *J. Organomet. Chem.* **1992**, *441*, 499 and references cited therein. (15) Jeffery, J. C.; Jelliss, P. A.; Stone, F. G. A. *Inorg. Chem.* **1993**, *32*, 3943.

Table 4. Selected Internuclear Distances (Å) and Angles (deg) for [PtAu(PEt₃)₂(PPh₃)(η⁵-7-CB₁₀H₁₁)] (**3a**) with Estimated Standard Deviations in Parentheses

Au-P(2)	2.243(2)	Au-Pt	2.6112(7)	Pt-B(2)	2.238(6)	Pt-B(1)	2.259(6)
Pt-P(1)	2.3487(14)	Pt-C	2.387(7)	P(1)-C(3)	1.972(14)	P(1)-C(1)	1.781(11)
P(1)-C(5)	1.822(6)	B(1)-B(4)	1.769(9)	B(1)-B(5)	1.784(8)	P(2)-C(21)	1.818(5)
P(2)-C(31)	1.830(8)	B(2)-C	1.708(8)	B(2)-B(5)	1.775(9)	B(1)-B(1A)	1.804(12)
B(1)-B(2)	1.863(9)	B(4)-B(7)	1.755(12)	B(4)-B(5)	1.768(9)	B(2)-B(6)	1.802(9)
C-B(6)	1.680(9)	B(5)-B(7)	1.781(8)	B(6)-B(6A)	1.75(2)	B(4)-B(1A)	1.769(9)
B(5)-B(6)	1.776(10)	B(6)-B(7)	1.759(10)				
P(2)-Au-Pt	167.51(5)	B(2A)-Pt-B(2)	76.8(3)	B(2)-Pt-B(1)			49.0(2)
B(2)-Pt-B(1A)	80.7(2)	B(1A)-Pt-B(1)	47.1(3)	B(2A)-Pt-P(1)			152.8(2)
B(2)-Pt-P(1)	86.9(2)	B(1A)-Pt-P(1)	149.5(2)	B(1)-Pt-P(1)			104.8(2)
P(1)-Pt-P(1A)	98.99(8)	B(2)-Pt-C	43.2(2)	B(1)-Pt-C			78.0(2)
P(1)-Pt-C	110.97(11)	B(2)-Pt-Au	118.6(2)	B(1)-Pt-Au			73.83(14)
P(1)-Pt-Au	88.27(4)	C-Pt-Au	149.2(2)	C(1)-P(1)-C(5)			113.0(5)
C(1)-P(1)-C(3)	97.8(7)	C(5)-P(1)-C(3)	98.6(6)	C(1)-P(1)-Pt			115.1(4)
C(5)-P(1)-Pt	115.9(2)	C(3)-P(1)-Pt	113.8(5)	C(21)-P(2)-C(31)			106.2(2)
C(21)-P(2)-Au	116.7(2)	C(31)-P(2)-Au	108.4(2)	C-B(2)-Pt			73.1(3)
B(2)-C-Pt	63.7(3)						

Table 5. Selected Internuclear Distances (Å) and Angles (deg) for [PtCu(PEt₃)₂(PPh₃)(η⁵-7-CB₁₀H₁₁)] (**3b**) with Estimated Standard Deviations in Parentheses

Pt-B(2)	2.251(3)	Pt-B(4)	2.265(3)	Pt-B(5)	2.270(3)	Pt-B(3)	2.284(4)
Pt-P(1)	2.3169(8)	Pt-P(2)	2.3187(8)	Pt-C(1)	2.449(3)	Pt-Cu	2.6058(5)
Cu-P(3)	2.1923(9)	Cu-B(3)	2.258(4)	Cu-B(4)	2.268(4)	Cu-H(3)	2.00(4)
Cu-H(4)	2.09(4)	C(1)-B(7)	1.660(5)	C(1)-B(6)	1.675(5)	C(1)-B(5)	1.679(5)
C(1)-B(2)	1.715(5)	B(2)-B(8)	1.796(6)	B(2)-B(7)	1.798(5)	B(2)-B(3)	1.846(6)
B(3)-B(8)	1.769(5)	B(3)-B(9)	1.786(6)	B(4)-B(10)	1.772(5)	B(4)-B(9)	1.784(5)
B(4)-B(5)	1.880(5)	B(5)-B(10)	1.793(5)	B(5)-B(6)	1.794(5)	B(6)-B(7)	1.762(5)
B(6)-B(10)	1.777(5)	B(6)-B(11)	1.781(5)	B(7)-B(11)	1.773(5)	B(7)-B(8)	1.785(6)
B(8)-B(9)	1.769(6)	B(8)-B(11)	1.788(5)	B(9)-B(11)	1.753(5)	B(9)-B(10)	1.772(6)
B(10)-B(11)	1.798(6)	P(1)-C(4)	1.827(3)	P(1)-C(2)	1.827(3)	P(1)-C(6)	1.845(3)
P(2)-C(8)	1.820(3)	P(2)-C(10)	1.830(3)	P(2)-C(12)	1.834(3)	P(3)-C(41)	1.823(3)
P(3)-C(31)	1.824(3)	P(3)-C(21)	1.824(3)				
B(2)-Pt-B(4)	79.45(14)	B(2)-Pt-B(5)	75.07(13)	B(4)-Pt-B(5)			48.99(13)
B(2)-Pt-B(3)	48.03(14)	B(4)-Pt-B(3)	46.98(14)	B(5)-Pt-B(3)			80.18(13)
B(2)-Pt-P(1)	161.68(10)	B(4)-Pt-P(1)	102.06(10)	B(5)-Pt-P(1)			92.01(9)
B(3)-Pt-P(1)	143.56(11)	B(2)-Pt-P(2)	86.09(10)	B(4)-Pt-P(2)			151.51(10)
B(5)-Pt-P(2)	148.51(9)	B(3)-Pt-P(2)	105.76(11)	P(1)-Pt-P(2)			99.35(3)
B(2)-Pt-C(1)	42.55(12)	B(4)-Pt-C(1)	76.32(11)	B(5)-Pt-C(1)			41.47(12)
B(3)-Pt-C(1)	76.58(12)	P(1)-Pt-C(1)	119.63(8)	P(2)-Pt-C(1)			108.76(8)
B(2)-Pt-Cu	101.68(11)	B(4)-Pt-Cu	54.98(9)	B(5)-Pt-Cu			54.53(10)
P(1)-Pt-Cu	93.81(2)	P(2)-Pt-Cu	105.20(2)	C(1)-Pt-Cu			126.20(7)
P(3)-Cu-B(3)	149.45(10)	P(3)-Cu-B(4)	149.12(9)	B(3)-Cu-B(4)			47.23(14)
P(3)-Cu-Pt	148.81(3)	B(3)-Cu-Pt	55.45(9)	B(4)-Cu-Pt			54.86(9)
P(3)-Cu-H(3)	122.4(12)	B(3)-Cu-H(3)	28.1(12)	B(4)-Cu-H(3)			73.8(12)
Pt-Cu-H(3)	75.7(12)	P(3)-Cu-H(4)	119.9(11)	B(3)-Cu-H(4)			74.9(11)
B(4)-Cu-H(4)	29.9(10)	Pt-Cu-H(4)	77.2(11)	H(3)-Cu-H(4)			98(2)

found (2.577(3)–2.735(3) Å) in cluster compounds in which a copper atom triply bridges a Pt₃ unit.¹⁶

Atoms H(3) and H(4) were located and their positions refined, affording parameters Cu–B(3) = 2.258(4), Cu–B(4) = 2.268(4), Cu–H(3) = 2.00(4), Cu–H(4) = 2.09(4), B(3)–H(3) = 1.06(4), and B(4)–H(4) = 1.14(4) Å. The two B–H→Cu bonds involve the BH groups which are β to the carbon in the CBBB ring coordinated to the platinum. The existence of exopolyhedral B–H→Cu bonding from an icosahedral fragment to copper has been observed previously in the anion of the complex [NEt₄][W₂Cu(μ-CC≡CBu^t)₂(CO)₄(η⁵-7,8-Me₂-7,8-C₂B₉H₉)₂] where one B–H→Cu linkage is present with Cu–H, Cu–B, and B–H distances of 1.78(10), 2.33(1), and 1.1(1) Å, respectively.¹⁷ As would be anticipated there are some similarities in the NMR spectra of **3a,3b**. Both species display diagnostic signals for the cage CH group in their ¹H (δ 2.77, **3a**; 2.93, **3b**) and ¹³C{¹H} (δ 48.2, **3a**; 52.8, **3b**) spectra. These

resonances are all broad as generally occurs in the spectra of metallocarboranes due to the quadrupolar effect of the boron. For these species the broadening is probably enhanced by the ⁶³Cu and ¹⁹⁷Au nuclei with spin *I* = 3/2. Diagnostic resonances for the B–H→Cu groups were not observed in the ¹H or ¹¹B-{¹H} spectra of **3b** in the expected regions δ –5.5 to –11 and δ 10–30, respectively.¹⁸ The absence of these signals may be due to exchange processes between the structure found in the solid state having B_β–H→Cu interactions and those in which these interactions are lifted and then rapidly re-form to the structure found in the crystal or equilibrate between some combination of B_α–H→Cu and B_β–H→Cu bonds.¹⁹ The exchange process between such structures would be of low energy and thus account for peaks due to B–H→Cu groups not being observed, even when the spectra were recorded at –90 °C. Alternatively, the signals may be so broadened they are lost in the background noise. Interestingly, resonances (¹H, ¹¹B{¹H}) for the B–H→Cu bond in [NEt₄][W₂Cu(μ-CC≡CBu^t)₂-

(16) (a) Hallam, M. F.; Mingos, D. M. P.; Adatia, T.; McPartlin, M. J. *Chem. Soc., Dalton Trans.* **1988**, 335. (b) Braunstein, P.; Freyburger, S.; Bars, O. *J. Organomet. Chem.* **1988**, 352, C29.

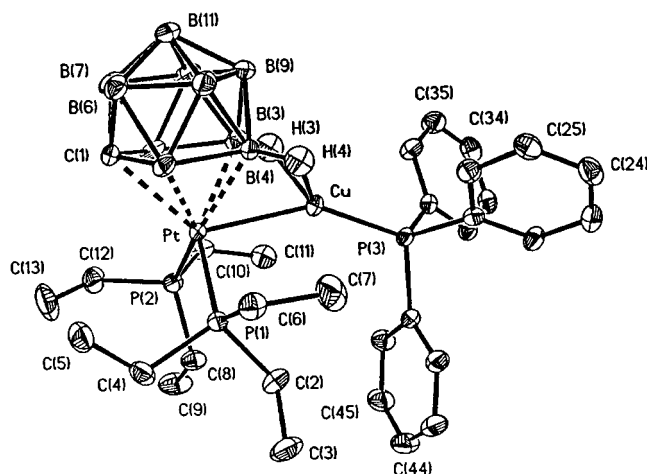
(17) Cabioch, J.-L.; Dossett, S. J.; Hart, I. J.; Pilotti, M. U.; Stone, F. G. A. *J. Chem. Soc., Dalton Trans.* **1991**, 519.

(18) Brew, S. A.; Stone, F. G. A. *Adv. Organomet. Chem.* **1993**, 35, 135.

(19) Jeffery, J. C.; Ruiz, M. A.; Sherwood, P.; Stone, F. G. A. *J. Chem. Soc., Dalton Trans.* **1989**, 1845.

Table 6. Selected Internuclear Distances (Å) and Angles (deg) for [PtHg(Ph)(PEt₃)₂(η⁵-7-CB₁₀H₁₁)] (**3c**) with Estimated Standard Deviations in Parentheses

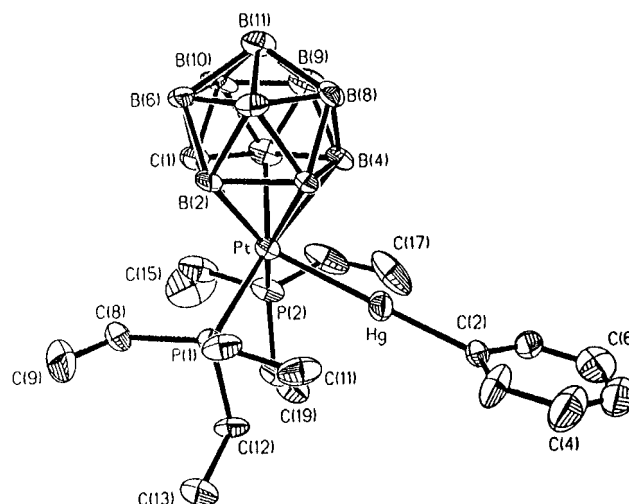
Pt–B(3)	2.237(12)	Pt–B(5)	2.256(12)	Pt–B(2)	2.258(12)	Pt–B(4)	2.324(11)
Pt–C(1)	2.350(9)	Pt–P(1)	2.355(3)	Pt–P(2)	2.359(3)	Pt–Hg	2.5850(5)
Hg–C(2)	2.17(2)	P(1)–C(8)	1.821(6)	P(1)–C(10)	1.828(10)	P(1)–C(12)	1.828(12)
P(2)–C(14)	1.786(13)	P(2)–C(16)	1.832(13)	P(2)–C(18)	1.870(12)	C(1)–B(6)	1.66(2)
C(1)–B(10)	1.66(2)	C(1)–B(2)	1.70(2)	C(1)–B(5)	1.70(2)	B(2)–B(6)	1.74(2)
B(2)–B(7)	1.79(2)	B(2)–B(3)	1.87(2)	B(3)–B(8)	1.80(2)	B(3)–B(7)	1.83(2)
B(3)–B(4)	1.858(14)	B(4)–B(9)	1.74(2)	B(4)–B(8)	1.77(2)	B(4)–B(5)	1.85(2)
B(5)–B(9)	1.76(2)	B(5)–B(10)	1.80(2)	B(6)–B(10)	1.71(2)	B(6)–B(7)	1.78(2)
B(6)–B(11)	1.80(2)	B(7)–B(8)	1.76(2)	B(7)–B(11)	1.80(2)	B(8)–B(11)	1.755(14)
B(8)–B(9)	1.80(2)	B(9)–B(11)	1.79(2)	B(9)–B(10)	1.79(2)	B(10)–B(11)	1.72(2)
B(3)–Pt–B(5)	80.9(4)	B(3)–Pt–B(2)	49.2(4)	B(5)–Pt–B(2)	76.8(4)		
B(3)–Pt–B(4)	48.0(4)	B(5)–Pt–B(4)	47.7(5)	B(2)–Pt–B(4)	80.9(4)		
B(3)–Pt–C(1)	78.3(4)	B(5)–Pt–C(1)	43.3(4)	B(2)–Pt–C(1)	43.2(4)		
B(4)–Pt–C(1)	77.3(4)	B(3)–Pt–P(1)	103.0(3)	B(5)–Pt–P(1)	151.3(4)		
B(2)–Pt–P(1)	84.5(3)	B(4)–Pt–P(1)	149.6(2)	C(1)–Pt–P(1)	109.0(3)		
B(3)–Pt–P(2)	156.0(3)	B(5)–Pt–P(2)	85.7(3)	B(2)–Pt–P(2)	145.4(3)		
B(4)–Pt–P(2)	108.8(3)	C(1)–Pt–P(2)	105.1(3)	P(1)–Pt–P(2)	98.32(8)		
B(3)–Pt–Hg	78.7(3)	B(5)–Pt–Hg	121.0(4)	B(2)–Pt–Hg	123.1(3)		
B(4)–Pt–Hg	78.7(3)	C(1)–Pt–Hg	154.3(2)	P(1)–Pt–Hg	87.35(7)		
P(2)–Pt–Hg	91.5(1)	C(2)–Hg–Pt	171.2(5)				

**Figure 3.** Molecular structure of [PtCu(PEt₃)₂(PPh₃)(η⁵-7-CB₁₀H₁₁)] (**3b**), showing the crystallographic labeling scheme. Thermal ellipsoids are at the 40% probability level, and except for H(3) and H(4) the positions of which were located and refined, hydrogen atoms are omitted for clarity.

(CO)₄(η⁵-7,8-Me₂-7,8-C₂B₉H₉O₂) were also not seen in the NMR spectra of this complex.¹⁷

The establishment of the presence of B–H→Cu linkages in **3b** and the absence of B–H→Au interactions in the gold analog **3a** is of interest. This must relate to the distinct preference of copper(I) to adopt a tetrahedral coordination whereas gold(I) prefers a linear coordination. This difference in geometries stems from relative differences in the energies of the unoccupied frontier orbitals in the fragments M(PPh₃) (M = Cu or Au). For copper the valence hybrid sp_z orbital and the degenerate pair of p_x and p_y orbitals are sufficiently close to make all three orbitals valence orbitals whereas with gold the p_x and p_y orbitals are of much higher energy and therefore are less accessible for bonding, a feature discussed elsewhere.²⁰

The reaction between **1a** and [HgClPh] in thf was next investigated and found to yield yellow crystals of the dimetal complex [PtHg(Ph)(PEt₃)₂(η⁵-7-CB₁₀H₁₁)] (**3c**), which was characterized both by the data given in Tables 1 and 2 and by a single-crystal X-ray diffraction study. The molecule is shown in Figure 4, and selected bond distances and angles are given in Table 6. Overall the structure resembles those of **2** and **3a** with the HgPh group replacing the H and Au(PPh₃) moieties,

**Figure 4.** Molecular structure of [PtHg(Ph)(PEt₃)₂(η⁵-7-CB₁₀H₁₁)] (**3c**), showing the crystallographic labeling scheme. Thermal ellipsoids are at the 40% probability level, and hydrogen atoms are omitted for clarity.

respectively, and the CB₁₀H₁₁ cage coordinated to the Pt atom in the usual manner. The metal–metal bond distance of 2.5850(5) Å is at the shorter end of the range found (2.5–2.8 Å) for such separations in a variety of Pt–Hg compounds.²¹ The Pt–Hg–C(Ph) group (Pt–Hg–C(2) = 171.2(5)°) is somewhat more linear than the Pt–Au–PPh₃ group (Pt–Au–P(2) = 167.51(5)°) in **3a**. However, not surprisingly due to the ability of the copper atom in **3b** to adopt a tetrahedral geometry the Pt–Cu–PPh₃ group in **3b** is far from linear (Pt–Cu–P(3) = 148.8(1)°).

The NMR data for **3c** (Table 3) are in accord with the structure established by X-ray diffraction. Broad resonances for the CH group are seen in the ¹H NMR spectrum δ 2.80 and in the ¹³C{¹H} spectrum at δ 59.3. The ³¹P{¹H} NMR spectrum shows a singlet at δ 0.77 for the equivalent PEt₃ ligands with ¹⁹⁵Pt and ²⁰¹Hg satellite peaks (*J* = 2259 and 188 Hz, respectively).

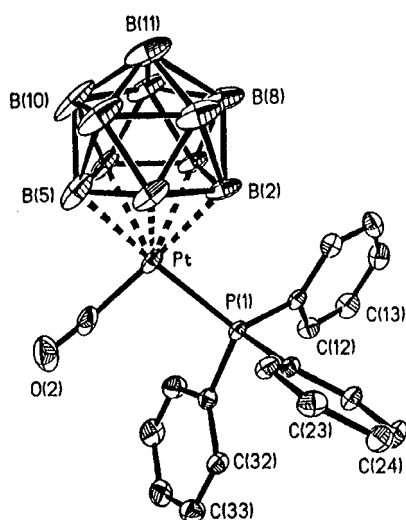
During the course of the work described herein, the reaction between [Na]₃[CB₁₀H₁₁] and [PtCl₂(CO)(PPh₃)] was investigated. Addition of [N(PPh₃)₂]Cl to the mixture gave the

(21) (a) Toronto, D. V.; Balch, A. L. *Inorg. Chem.* **1994**, *33*, 6132. (b) Krumm, M.; Zangrando, E.; Randaccio, L.; Menzer, S.; Danzmann, A.; Holthenrich, D.; Lippert, B. *Inorg. Chem.* **1993**, *32*, 2183 and references cited therein.

(20) Hamilton, E. J. M.; Welch, A. J. *Polyhedron* **1990**, *9*, 2407.

Table 7. Selected Internuclear Distances (Å) and Angles (deg) for $[\text{N}(\text{PPh}_3)_2][\text{Pt}(\text{CO})(\text{PPh}_3)(\eta^5\text{-7-CB}_{10}\text{H}_{11})]$ (**4**) with Estimated Standard Deviations in Parentheses

Pt—C(2)	1.865(6)	Pt—B(3)	2.248(5)	Pt—B(2)	2.260(6)	Pt—B(4)	2.265(5)
Pt—B(5)	2.267(5)	Pt—P(1)	2.3093(10)	Pt—C(1)	2.468(5)	P(1)—C(31)	1.825(4)
P(1)—C(21)	1.827(4)	P(1)—C(11)	1.834(4)	C(2)—O(2)	1.156(7)	C(1)—B(6)	1.666(7)
C(1)—B(7)	1.678(10)	C(1)—B(5)	1.712(9)	C(1)—B(2)	1.679(7)	B(2)—B(7)	1.816(7)
B(2)—B(8)	1.829(8)	B(2)—B(3)	1.910(7)	B(3)—B(9)	1.765(7)	B(3)—B(8)	1.784(8)
B(3)—B(4)	1.786(9)	B(4)—B(9)	1.771(11)	B(4)—B(10)	1.795(9)	B(4)—B(5)	1.898(7)
B(5)—B(10)	1.811(9)	B(5)—B(6)	1.822(11)	B(6)—B(7)	1.743(12)	B(6)—B(10)	1.777(9)
B(6)—B(11)	1.780(11)	B(7)—B(11)	1.780(9)	B(7)—B(8)	1.795(8)	B(8)—B(11)	1.775(9)
B(8)—B(9)	1.777(11)	B(9)—B(10)	1.754(10)	B(9)—B(11)	1.765(9)	B(10)—B(11)	1.784(13)
C(2)—Pt—B(3)	143.0(2)	C(2)—Pt—B(2)	162.4(2)	B(3)—Pt—B(2)	50.1(2)		
C(2)—Pt—B(4)	102.8(2)	B(3)—Pt—B(4)	46.6(2)	B(2)—Pt—B(4)	81.2(2)		
C(2)—Pt—B(5)	94.1(3)	B(3)—Pt—B(5)	80.2(2)	B(2)—Pt—B(5)	75.3(3)		
B(4)—Pt—B(5)	49.5(2)	C(2)—Pt—P(1)	94.2(2)	B(3)—Pt—P(1)	103.6(1)		
B(2)—Pt—P(1)	91.9(1)	B(4)—Pt—P(1)	144.7(1)	B(5)—Pt—P(1)	160.0(2)		
C(2)—Pt—C(1)	122.3(2)	B(3)—Pt—C(1)	76.7(2)	B(2)—Pt—C(1)	41.3(2)		
B(4)—Pt—C(1)	77.2(2)	B(5)—Pt—C(1)	42.1(2)	P(1)—Pt—C(1)	118.9(1)		
C(31)—P(1)—C(21)	103.9(2)	C(31)—P(1)—C(11)	103.3(2)	C(21)—P(1)—C(11)	102.7(2)		
C(31)—P(1)—Pt	112.0(1)	C(21)—P(1)—Pt	115.4(1)	C(11)—P(1)—Pt	117.8(1)		
O(2)—C(2)—Pt	175.8(4)						

**Figure 5.** Structure of the anion $[\text{Pt}(\text{CO})(\text{PPh}_3)(\eta^5\text{-7-CB}_{10}\text{H}_{11})]^-$ of **4**, showing the crystallographic labeling scheme. Thermal ellipsoids are at the 40% probability level, and hydrogen atoms are omitted for clarity.

expected product $[\text{N}(\text{PPh}_3)_2][\text{Pt}(\text{CO})(\text{PPh}_3)(\eta^5\text{-7-CB}_{10}\text{H}_{11})]$ (**4**) but only in poor yield. Data for this salt are given in Tables 1 and 2, and the results of an X-ray diffraction study are summarized in Table 7. The anion is shown in Figure 5. The platinum atom is coordinated on one side by the open face of the *nido*- $\text{CB}_{10}\text{H}_{11}$ cage (Pt—C(1) = 2.468(5), Pt—B(2) = 2.260(6), Pt—B(3) = 2.248(5), Pt—B(4) = 2.265(5), Pt—B(5) = 2.267(5) Å) and on the other by the PPh_3 (Pt—P(1) = 2.309(1) Å) and CO (Pt—C(2) = 1.865(6) Å) groups. Hence in the anion the platinum adopts a pseudo-trigonal bipyramidal geometry if the $\eta^5\text{-CB}_{10}\text{H}_{11}$ ligand is assumed to occupy three coordination sites. The metal to *nido*-cage connectivities are similar to those in the other complexes studied.

Conclusions

The reactions of **1a** reported herein appear to be the first in which a monocarbon metallacarborane with an *closo*-icosahedral framework has been used as a reagent to prepare compounds with various groups attached exopolyhedrally to the metal atom of the MCB_{10} cage system. In the complexes **2**, **3a,c**, and **4** the *nido*- $\text{CB}_{10}\text{H}_{11}$ group adopts a spectator role, functioning formally as a three electron donor to the platinum with the open CBBBB face of the cage coordinated to the metal. However, in the platinum–copper complex **3b** the PtCB_{10} cage is attached

to the exopolyhedral copper atom both by a Pt—Cu bond and by donation of electron pairs from two of the B—H bonds. These

boron atoms lie in the CBBBB ring ligating the platinum. This would appear to be the first example of a compound where a monocarbon carborane ligand behaves in this noninnocent manner.

Experimental Section

General Considerations. Experiments were conducted under an atmosphere of dry nitrogen or argon using Schlenk-line techniques. Solvents were freshly distilled under nitrogen from appropriate drying agents before use. Light petroleum refers to that fraction of boiling point 40–60 °C. Tetrahydrofuran was distilled from potassium–benzophenone under nitrogen and stored over Na/K alloy. Chromatography columns (ca. 30 cm long and 3 cm in diameter) were packed under nitrogen with silica gel (Acros, 70–230 mesh). NMR spectra were recorded in CD_2Cl_2 at the following frequencies: ^1H at 360.13, ^{13}C at 90.6, ^{11}B at 115.3, and ^{31}P at 145.8 MHz. The salt $[\text{Na}]_3[\text{CB}_{10}\text{H}_{11}]$ was synthesized from 7- $\text{Me}_3\text{N-7-CB}_{10}\text{H}_{12}$ according to the method of Knoth *et al.*⁹ The complexes $[\text{AuCl}(\text{PPh}_3)]_2$ ²² and $[\text{CuCl}(\text{PPh}_3)]_4$ ²³ were prepared according to the literature methods, and $[\text{HgClPh}]$ was purchased from Aldrich.

Synthesis of the Alkali Metal Salts $[\text{M}][\text{Pt}(\text{PET}_3)_2(\eta^5\text{-7-CB}_{10}\text{H}_{11})]$ [$\text{M} = \text{Na}, \text{K}$]. In a typical preparation, 7- $\text{Me}_3\text{N-7-CB}_{10}\text{H}_{12}$ (0.19 g, 1.00 mmol) was dissolved in dry thf (15 mL) and three small pieces of freshly cut sodium metal (ca. 0.30 g) were added. Once the evolution of hydrogen had ceased, the mixture was refluxed under nitrogen for 24 h to yield a thick white precipitate of $[\text{Na}]_3[\text{CB}_{10}\text{H}_{11}]$. After cooling of the mixture to room temperature, the excess sodium was removed and the precipitate was cooled to –96 °C using a toluene–liquid nitrogen bath. A suspension of $[\text{PtCl}_2(\text{PET}_3)_2]$ (0.50 g, 0.99 mmol) in thf (20 mL) was added via a syringe and the mixture warmed to room temperature over a period of 1 h. During this time the thick white precipitate became orange-brown in color. The mixture was then warmed at 50 °C for 1 h giving a moderately clear, orange-brown solution containing $[\text{Na}][\text{Pt}(\text{PET}_3)_2(\eta^5\text{-7-CB}_{10}\text{H}_{11})]$ (**1a**). This reagent was normally used *in situ* without purification in order to avoid its ready hydrolysis. The impurity is ca. 2–5% of $[\text{Na}][\text{nido-CB}_{10}\text{H}_{13}]$.

Alternatively, freshly cut and washed potassium metal (0.12 g, 3.00 mmol) was added to rapidly stirred dry thf (15 mL), and the solution treated with 7- $\text{Me}_3\text{N-7-CB}_{10}\text{H}_{12}$ (0.19 g, 1.00 mmol). Stirring was continued for 10 min at room temperature giving a thick white precipitate after which the mixture was refluxed for 4 h and a suspension of $[\text{PtCl}_2(\text{PET}_3)_2]$ (0.50 g, 0.99 mmol) in thf (20 mL) was added. The dark brown thf solution of $[\text{K}][\text{Pt}(\text{PET}_3)_2(\eta^5\text{-7-CB}_{10}\text{H}_{11})]$ (**1b**) thus obtained was cooled to –96 °C and used *in situ*.

(22) Bruce, M. I.; Nicholson, B. K.; Bin-Shawkataly, O. *Inorg. Synth.* **1989**, 26, 325.

(23) Jardine, F. H.; Rule, J.; Vohra, A. G. *J. Chem. Soc. A* **1970**, 238.

Table 8. Data for X-ray Crystal Structure Analyses

	2	3a	3b	3c·0.5H₂O	4·CH₂Cl₂
cryst dimens (mm)	0.15 × 0.24 × 0.27	0.50 × 0.30 × 0.25	0.30 × 0.30 × 0.25	0.50 × 0.20 × 0.20	0.55 × 0.45 × 0.24
formula	C ₁₃ H ₄₃ B ₁₀ OP ₂ Pt	C ₃₁ H ₅₆ AuB ₁₀ P ₃ Pt	C ₃₁ H ₅₆ B ₁₀ CuP ₃ Pt	C ₁₉ H ₄₇ B ₁₀ HgO _{0.5} P ₂ Pt	C ₅₇ H ₅₆ B ₁₀ Cl ₂ NOP ₃ Pt
<i>M_r</i>	581.6	1021.82	888.40	849.29	1240.04
cryst color, shape	colorless parallelepiped	pale yellow block	pale yellow block	yellow needle	orange block
cryst system	monoclinic	orthorhombic	monoclinic	tetragonal	monoclinic
space group	<i>P</i> ₂ / <i>c</i>	<i>Pnma</i>	<i>P</i> ₂ / <i>n</i>	<i>P</i> ₄ ₂ <i>2</i> ₁	<i>P</i> ₂ / <i>c</i>
<i>T</i> /K	295	173	173	173	173
<i>a</i> /Å	18.656(3)	18.597(2)	12.480(2)	18.491(4)	10.712(2)
<i>b</i> /Å	15.877(3)	15.591(3)	19.244(3)	18.491(4)	32.048(7)
<i>c</i> /Å	18.392(3)	12.932(4)	16.046(4)	17.450(3)	16.683(3)
<i>β</i> /deg	116.467(11)		91.682(11)		95.833(11)
<i>V</i> /Å ³	5019.9(13)	3826.2(14)	3852.0(11)	5966(2)	5697(2)
<i>Z</i>	4	4	4	8	4
<i>d</i> _{calc} /g cm ⁻³	1.515	1.769	1.532	1.891	1.446
<i>μ</i> (Mo Kα)/cm ⁻¹	5.774	7.610	4.327	9.942	2.682
<i>F</i> (000) (e)	2264	1976	1776	3224	2488
2θ range (deg)	3–40	5–50	5–50	5–50	5–50
no. of reflcns measd	5104	17 521	18 069	28 378	26 580
no. of unique reflcns	4676	3524	6741	5264	9965
no. of obsd reflcns	4096				
criterion for obsd, <i>n</i> [<i>F</i> _o ≥ <i>nσ</i> (<i>F</i> _o)]	4				
reflcn limits					
<i>h</i>	0 to 17	–22 to 21	–12 to 14	–21 to 21	–12 to 12
<i>k</i>	0 to 15	–18 to 13	22 to –22	–21 to 19	–38 to 34
<i>l</i>	–18 to 16	–15 to 15	–19 to 18	–20 to 13	–19 to 18
final residuals	<i>R</i> = 0.0317 (<i>R</i> ' = 0.0409) ^a	<i>wR</i> ₂ = 0.0831 (<i>R</i> ₁ = 0.0279) ^b	<i>wR</i> ₂ = 0.0532 (<i>R</i> ₁ = 0.0205) ^b	<i>wR</i> ₂ = 0.0785 (<i>R</i> ₁ = 0.0345) ^b	<i>wR</i> ₂ = 0.0752 (<i>R</i> ₁ = 0.0337) ^b
weighting factors	<i>g</i> = 0.001	<i>a</i> = 0.0380, <i>b</i> = 10.033 ^b	<i>a</i> = 0.0222, <i>b</i> = 3.802 ^b	<i>a</i> = 0.0187, <i>b</i> = 43.30 ^b	<i>a</i> = 0.0196, <i>b</i> = 17.2266 ^b
final electron density diff features (max/min)/e Å ⁻³	1.87/–0.77	1.39/–1.15	0.43/–0.79	2.02/–1.38	1.36/–1.54
goodness of fit	1.30	1.117	1.164	0.96	1.122

^a Refinement was by block full-matrix least-squares on *F* data with a weighting scheme of the form $w^{-1} = [\sigma^2(F_o) + g|F_o|^2]$, where $\sigma_c^2(F_o)$ is the variance in *F*_o due to counting statistics: $R = \sum ||F_o| - |F_c|| / \sum |F_o|$, $R' = \sum w^{1/2} ||F_o| - |F_c|| / \sum w^{1/2} |F_o|$. ^b Refinement was full-matrix least-squares on all *F*² data: $wR_2 = [\sum [w(F_o^2 - F_c^2)^2] / \sum w(F_o^2)^2]^{1/2}$, where $w = [\sigma^2(F_o^2) + (aP)^2 + bP]$ and $P = [\max(F_o^2, 0) + 2F_c^2] / 3$. The value in parentheses is given for comparison with refinements based on *F*_o with a typical threshold of $F \geq 4\sigma(F)$ and $R_1 = \sum ||F_o| - |F_c|| / \sum |F_o|$, $R' = \sum w^{1/2} ||F_o| - |F_c|| / \sum w^{1/2} |F_o|$ and $w^{-1} = [\sigma^2(F_o) + g|F_o|^2]$.

Synthesis of [PtH(PEt₃)₂(η⁵-7-CB₁₀H₁₁)]. Method i. The acid HBF₄·Et₂O (147 μL, 1.00 mmol) was added to a rapidly stirred solution of **1a** (1.00 mmol) prepared in thf (20 mL) as above and cooled to ca. –96 °C. Upon warming of the mixture to room temperature, a yellow-brown solution formed which was stirred overnight. Solvent was removed *in vacuo* and CH₂Cl₂ (20 mL) added to dissolve the residue. Filtration through a Celite pad gave a clear, light brown solution which was chromatographed. Elution with CH₂Cl₂–light petroleum (1:1) afforded a pale brown-yellow fraction. Removal of solvent *in vacuo* followed by crystallization of the residue from CH₂Cl₂–Et₂O (1:4) gave colorless crystals of [PtH(PEt₃)₂(η⁵-7-CB₁₀H₁₁)] (0.24 g) (**2**).

Method ii. In a similar reaction, a solution of **1a** (1.00 mmol) in thf (20 mL) at ca. –95 °C was treated with a 1 M solution of HCl in diethyl ether (1.0 mL, 1.0 mmol). The same workup procedure again yielded **2**.

Synthesis of the Platinum–Gold, –Copper, and –Mercury Complexes. Method i. A solution of [AuCl(PPh₃)] (0.25 g, 0.50 mmol) in thf (20 mL) was added using a syringe to a chilled (ca. –96 °C) thf (20 mL) solution of compound **1a** (0.50 mmol). After warming of the solution to room temperature and stirring for 2 h, solvent was removed *in vacuo* and the dark yellow residue taken up in CH₂Cl₂ (50 mL) and filtered through a Celite pad. The volume of solution was reduced *in vacuo* to ca. 5 mL and cooled to 0 °C giving a white precipitate which was allowed to settle. Solvent was removed with a syringe and the residue pumped dry *in vacuo*. Crystallization from CH₂Cl₂–petroleum (1:4, 10 mL) gave pale yellow crystals of [PtAu-(PEt₃)₂(PPh₃)(η⁵-7-CB₁₀H₁₁)] (0.49 g) (**3a**).

Method ii. Similarly, a thf solution (15 mL) of [CuCl(PPh₃)₄] (0.18 g, 0.50 mmol) was added via a syringe to a chilled (ca. –96 °C) solution of compound **1a** (0.50 mmol) in thf (20 mL). After being warmed to room temperature, the mixture was stirred at 40 °C for 2 h while a red precipitate formed. The red solid was removed by filtration, and the

filtrate was reduced in volume *in vacuo* to 3 mL. Chromatography, eluting with CH₂Cl₂–light petroleum (3:1), removed a pale yellow band. After removal of solvent the residue was crystallized from CH₂Cl₂–pentane (2:5, 10 mL) to yield pale yellow crystals of [PtCu(PEt₃)₂(PPh₃)(η⁵-7-CB₁₀H₁₁)] (0.32 g) (**3b**).

Method iii. A freshly prepared solution of **1a** (1.00 mmol) in thf (20 mL) was cooled to ca. –96 °C, and a solution of [HgClPh] (0.31 g, 1.00 mmol) in thf (15 mL) was added via a syringe. After being warmed to room temperature, an olive-green solution formed which was maintained at ca. 40 °C for 1 h. Solvent was removed *in vacuo*, and the residue extracted with CH₂Cl₂ (20 mL), and the extract filtered through a Whatman 1 μm pore size Paradisc PTFE membrane to give a clear yellow-green solution which was reduced in volume to ca. 3 mL. Addition of pentane (20 mL) gave an olive-yellow solid which was collected by filtration and crystallized from CH₂Cl₂–pentane to afford yellow *microcrystals* of [PtHg(Ph)(PEt₃)₂(η⁵-7-CB₁₀H₁₁)] (0.45 g) (**3c**).

Synthesis of [PPN][Pt(CO)(PPh₃)(η⁵-7-CB₁₀H₁₁)]. Addition of [PtCl₂(CO)(PPh₃)] (0.28 g, 0.50 mmol) in thf (20 mL) to a chilled solution of [Na][CB₁₀H₁₁] (0.50 mmol) prepared in thf (25 mL) gave, after warming to room temperature and stirring for 4 h, a deep brown solution. The solvent was removed *in vacuo* and the residue extracted with CH₂Cl₂ (50 mL) and passed through a Celite pad. The salt [N(PPh₃)₂Cl] (0.28 g, 0.50 mmol) was added to the solution and the mixture stirred overnight. After filtration, the volume of solvent was reduced to ca. 5 mL and cooled to 0 °C. Addition of light petroleum (20 mL) gave an orange precipitate which was redissolved in CH₂Cl₂, and the solution was chromatographed. Elution with CH₂Cl₂ afforded an orange band from which [PPN][Pt(CO)(PPh₃)(η⁵-7-CB₁₀H₁₁)] (**4**) was obtained (0.04 g) after removal of solvent.

Crystal Structure Determination and Refinements. Crystals were grown by diffusion of light petroleum into CH₂Cl₂ solutions of the

complexes. A conoscopic examination of **2**, using crystal rotation between crossed polarizers on a Zeiss Photomicroscope (II), verified the optical quality and biaxial nature of the system. A suitable single crystal was selected and attached to a glass fiber and mounted on an Enraf-Nonius CAD4-F autodiffractometer equipped with a dense graphite monochromator (take-off angle 2.8°). Final lattice parameters were determined by a least-squares refinement of 25 accurately centered high-angle reflections. The data were collected at room temperature in the ω - 2θ mode at a variable scan rate of 0.54 – $5.17^\circ \text{ min}^{-1}$. A decay of 4.6% dictated the use of the SDP program Decay²⁴ which applied a linear decay correction to the data set. After deletion of the check reflections and systematic absences, averaging of duplicate and equivalent measurements was performed and the data were corrected for Lorentz, polarization, and X-ray absorption effects. The latter corrections were based on numerical methods employing crystal face measurements.²⁵

Crystallographic analysis employing the heavy atom Patterson technique revealed the location of the Pt and P atoms and subsequent difference Fourier mapping located the remainder of the non-hydrogen atoms. Hydrogen H(1a) was located by employing the energy minimization program XHYDEX.¹⁰ All other hydrogen atoms were included in the refinement at geometrically calculated positions (C–H = 0.96 \AA and B–H = 1.10 \AA ²⁶) and were constrained to ride on their parent carbon, platinum, or boron atoms with fixed isotropic thermal parameters ($U_{\text{iso}} = 80 \times 10^{-3}$, 80×10^{-3} , and $60 \times 10^{-3} \text{ \AA}^2$, respectively). After several cycles of full-matrix least-squares refinement of all non-hydrogen atoms, the structural model converged. All calculations were performed using the SHELXTL-PC package of programs^{27a} with atomic scattering factors taken from the usual source.²⁸

Data for **3a–c** and **4** (Table 8) were collected at 173 K on a Siemens SMART CCD area-detector 3-circle diffractometer using Mo K α X-radiation, $\lambda = 0.71073 \text{ \AA}$, with the crystals mounted on glass fibers. For three settings of ϕ , narrow data “frames” were collected for 0.3° increments in ω . A total of 1321 frames of data were obtained affording rather more than a hemisphere of data. At the end of the collection, the first 50 frames were recollected confirming that crystal decay had

not taken place during the course of data collection. The substantial redundancy in data allows empirical absorption corrections to be applied using multiple measurements of equivalent reflections. Data frames were collected for 20 s per frame. The data frames were integrated using SAINT,^{27b} and the structures were solved by conventional direct methods. Refinement was by full-matrix least-squares on all F^2 data using Siemens SHELXTL version 5.03,^{27c} with anisotropic thermal parameters for all non-hydrogen atoms. Hydrogen atoms were included in calculated positions and allowed to ride on the parent boron or carbon atoms with isotropic thermal parameters ($U_{\text{iso}} = 1.2 \times U_{\text{iso equiv}}$ of the parent atom except for Me protons where $U_{\text{iso}} = 1.5 \times U_{\text{iso equiv}}$). However, for **3b** atoms H(3) and H(4) were located from final electron density difference syntheses and their positions were refined. In **3a** the molecule has imposed mirror symmetry with the Pt, Au, C(cage), and P(2) atoms lying on the mirror plane of symmetry. Two of the ethyl groups attached to P(1) [C(1)C(2) and C(3)C(4)] are disordered over two sites, and only one of these is shown in Figure 2. In **3c**, crystals of the complex are enantiomeric twins. In addition the Ph ring attached to the Hg atom is disordered (ca. 50:50) over two sites, only one of which is shown in Figure 4. It was not possible to resolve two sites for the Hg atom, and the Hg–Ph distances and angles should therefore be treated with caution. The asymmetric unit also contains half a molecule of H₂O which lies astride a 2-fold axis of symmetry. In **4** the asymmetric unit contains one molecule of the Pt anion and a well-defined molecule of the [PPN]⁺ counterion. The asymmetric unit also contains one molecule of CH₂Cl₂ which is disordered with one of the Cl atoms occupying two sites. The atoms of the carborane cage have unusually large anisotropic thermal parameters for a structure carried out at low temperature. This suggests that the cage may exhibit some disorder, but it was not possible to split the cage atoms into disordered components. The cage carbon atom C(1) was tentatively assigned on the basis of its bond lengths to adjacent boron atoms. However it is possible that this carbon site might be partially disordered among other sites in the ligated $\overline{\text{CBBBB}}$ face of the cage and this may account for the unusual anisotropic thermal parameters noted above. All calculations were carried out on Silicon Graphics Iris, Indigo, or Indy computers.

Acknowledgment. We thank the Robert A. Welch Foundation for support (Grants AA-1201 and -0668).

Supporting Information Available: Complete tables of atom coordinates, bond lengths and angles, anisotropic thermal parameters, and hydrogen atom parameters for **2**, **3a–c**, and **4** (49 pages). Ordering information is given on any current masthead page.

IC970042X

(24) Enraf-Nonius VAX Structure Determination Package, Delft, The Netherlands, 1989.

(25) Coppens, P.; Leiserowitz, L.; Rabinovich, D. *Acta Crystallogr.* **1965**, *18*, 1035.

(26) Sherwood P. BHGEN, a program for the calculation of idealized H-atom positions for a *nido*-icosahedral carborane cage, University of Bristol, 1986.

(27) (a) SHELXTL-PC, version 4.1. (b) SAINT. (c) SHELXTL, version 5.03, Siemens X-ray instruments, Madison, WI.

(28) *International Tables for X-ray Crystallography*; Kynoch Press: Birmingham, U.K., 1974; Vol. 4.